JOURNAL OF APPLIED ELECTROCHEMISTRY 11 (1981) 273–279

Electrical properties of pyrolytic MnO_2 layers

J. M. ALBELLA, L. FERNÁNDEZ-NAVARRETE, J. M. MARTÍNEZ-DUART

Departmento de Física Aplicada and Instituto Física Estado Sólido, CSIC, Universidad Autónoma Cantoblanco, Madrid, Spain

Received 19 June 1980

MnO_2 samples have been prepared by the pyrolytic decomposition of manganese nitrate in different atmospheres: dry air and air saturated with water vapour. The influence of the atmosphere on the kinetics of the manganese nitrate decomposition and on several physical properties of the resulting MnO_2, such as density, grain size, crystalline structure, resistivity and activation energy for electrical conduction, has been studied. The dielectric and breakdown properties of $Ta–Ta_2O_5–MnO_2$ capacitive structures, using MnO_2 as a solid electrolyte, are also strongly affected by the atmosphere in which the MnO_2 layers are prepared. It has been found that the electrical conductivity of the MnO_2 samples is greater when they are formed in a saturated water vapour atmosphere, resulting in substantially improved characteristics for the power losses and scintillation voltage of the corresponding tantalum capacitors.

1. Introduction

It is well known that the pyrolytic deposition of the MnO_2 layer in solid-electrolyte, tantalum capacitors with porous anodes results in a degradation of the electrical characteristics of the Ta_2O_5 dielectric. This effect can be attributed to various causes, among them the thermal treatment during the pyrolysis of the manganese nitrate, the formation of nitrous and water vapours as a consequence of the pyrolysis, and the presence of the MnO_2 itself [1–3]. Several procedures have been described in the literature to partially diminish these problems. One of the methods commonly employed in the capacitor industry consists of passing a flow of moist air through the oven in which the pyrolysis of the manganese nitrate is performed [4]. This results in tantalum capacitors with improved properties, especially lower power losses and better contacts [5]. However, there is a lack of published results on the electrical properties of the products resulting from the thermal decomposition of the manganese nitrate and on the influence, on the capacitor characteristics, of the properties of the MnO_2 layers obtained in wet or dry atmospheres [6].

2. Experimental results and discussion

The MnO_2 samples examined in this work were prepared by the thermal decomposition at 250° C of manganese nitrate ($Mn(NO_3)_2 \cdot 6H_2O$) in two kinds of ambient atmosphere: (a) in air, letting the vapours from the reaction escape freely from the oven, and (b) in air saturated with water vapour. In the latter case the oven was hermetically closed except for a small orifice to let the gases escape. In both cases, the time for the decomposition of the manganese nitrate was a minimum of two hours.

2.1. *Kinetics of the pyrolytic decomposition*

In order to determine the different stages of the pyrolytic decomposition of the manganese nitrate and the properties of the final product, the resistivity of the initial solution, as well as the products of the reaction, were determined throughout the whole process. The resisitivity was measured by means of a cell, with platinum electrodes, and a Hewlett Packard 4261-A LCR bridge at a frequency of 1 kHz. The platinum electrodes (size 5 mm × 5 mm, separation 2 mm) were fixed within the reaction cell which had a volume of approximately

0021–891X/81/030273–07$02.70/0

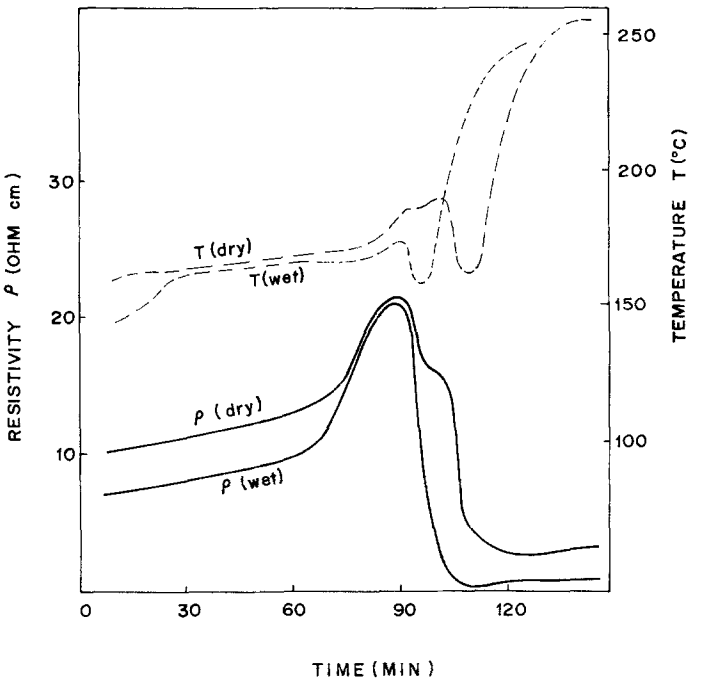

Fig. 1. Variation of resistivity (full lines) and temperature (broken lines) with time for humid and dry atmospheres during the manganese nitrate pyrolytic decomposition.

60 cm^3. The temperature was recorded by means of a sheathed thermocouple immersed in the cell close to the electrodes.

Fig. 1 shows the temperature of the cell and the resistivity during the thermal decomposition of the manganese nitrate in wet and dry atmospheres. In both cases the cell was introduced into the oven when the temperature was 100° C. The temperature of the oven was then raised to 250° C and at this temperature the measurement of the resistivity was initiated. As can be seen in Fig. 1 the curve showing the evolution of the resistivity with time is very similar for the moist and dry atmospheres. Three stages can be distinguished in these curves. These stages can be correlated with those found by Gallagher *et al.* [7–9] using thermogravimetry and differential thermal analysis techniques. The first step is dominated by the loss of the water of crystallization and during it the temperature and resistivity increase slowly. After about 75 minutes there is a rapid growth in resistivity and temperature of the solution which coincides with the end of the evaporation of the water molecules. In fact, the maximum in the resistivity curve should approximately correspond to the end of the transformation of the nitrate to oxynitrate $MnONO_3$ and the beginning of the MnO_2 formation by the decomposition of the unstable $MnONO_3$, which cannot be isolated. During the decomposition of the manganese nitrate a large amount of nitrous vapours is produced as by-products. Finally, the last section of the curves is characterized by a rapid decrease in the resistivity due to the large electrical conductivity of the MnO_2, which can be considered as a degenerate semiconductor. The minimum shown by the temperature curve is due to the absorption of heat during the MnO_2 formation. The rate of the reaction during this stage is much faster in moist air, the reason being the substantially lower activation energy for the reaction $MnONO_3 \rightarrow MnO_2 + NO_2$ in moist air [9]. In dry ambient air, the smaller rate of this reaction allows the detection of a shoulder in the resistivity curve (corresponding to a relative maximum in the temperature) which might be related to the formation of an intermediate crystalline phase of the MnO_2 before the end product is reached. Lastly, it is important to observe that the resistivity of the resulting MnO_2 is substantially lower when the pyrolysis is performed in air saturated with water vapour than in dry air.

2.2. *Structure*

The apparent density of the resulting MnO_2 was

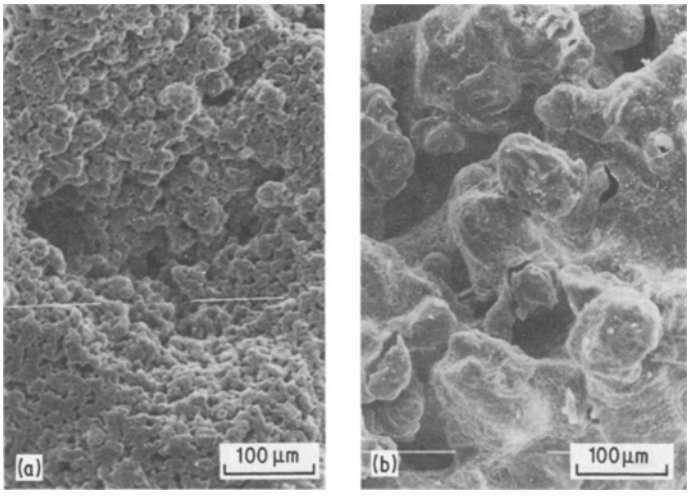

Fig. 2. SEM micrographs of the surface of the MnO_2 samples obtained in (a) humid and (b) dry atmospheres.

measured for the residue deposited at the bottom of the reaction cell in which the decomposition of the manganese nitrate was performed. The density obtained was $3.74 \pm 0.10\,g\,cm^{-3}$ for the samples formed in wet atmosphere and $3.3 \pm 0.10\,g\,cm^{-3}$ for those obtained in dry air. In both cases, the MnO_2 samples presented a higher degree of compaction in their interior than in their surface region, which was of a porous nature. Fig. 2 shows scanning electron micrographs of the surface region. From these it can be appreciated that sintering of the MnO_2 particles occurs to form granules, the grain size being approximately 12 and 100 μm for the samples obtained in wet and dry atmospheres respectively. This difference in grain size, besides explaining the differences in porosity, exerts a large influence in that part of the dielectric losses of the tantalum capacitors which are attributed to the cathodic contacts (see below).

X-ray structure determinations showed that the interior of the MnO_2 products obtained by pyrolytic deposition essentially consisted of the β-MnO_2 phase [10]. However, the surface region presented a high proportion of γ-MnO_2 (the most prominent phase in electrodeposited MnO_2 [11]) as can be seen in Table 1. The data in the table were obtained by the standard method for quantitative analysis of powder mixtures applied to the simple case of two polymorphic forms of the same substance. In this situation a linear relation is usually assumed to exist between the concentrations and the heights of the diffraction peaks. The approximations involved in this method are acceptable when comparing the relative concentrations of the MnO_2 phases in samples obtained under different conditions.

It can also be appreciated from this table that the thermal treatment of sample 1 in air induces the transformation of the γ-phase into the β-phase at the surface. A further thermal treatment of sample 1 to 580° C for 30 min transformed the MnO_2 into α-Mn_2O_3 [12].

2.3. *Resistivity*

The resistivity as a function of the temperature was measured in the MnO_2 samples as they were deposited in the same experimental set-up described above. In this way the properties of the MnO_2 layers can be related to those employed as solid electrolyte and cathodic contact in tantalum capacitors. The resistivity was measured with d.c. and with low frequency a.c., yielding practically identical values. The results are shown in Fig. 3 for four different samples. Samples 1 to 3 were given similar treatments to those described in Table 1. However sample 4, obtained in a wet atmosphere, underwent a thermal treatment to 650° C for one hour, thus becoming α-Mn_2O_3. The values of the room-temperature resistivity as well as the slopes of the curves in Fig. 3 are given in Table 2.

The conduction in nonstoichiometric β-MnO_2 is supposed to be due to oxygen vacancies pro-

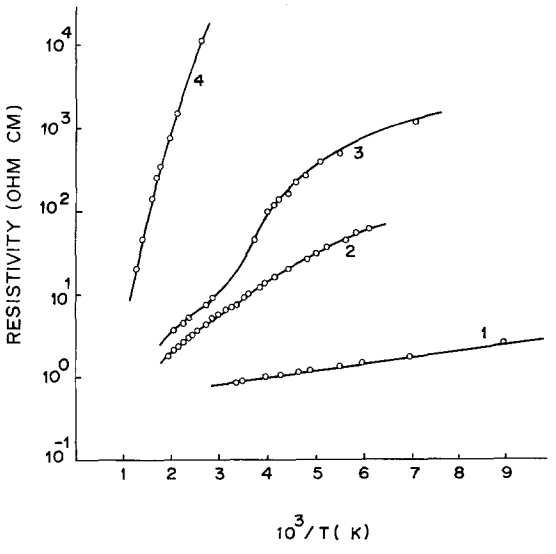

Fig. 3. Variation of resistivity with inverse absolute temperature (see text for the different curves).

ducing donor levels (n-type conduction) whose energy with respect to the bottom of the conduction band can be obtained from the slope of the $\log \rho$ versus $1/T$ curves of Fig. 3. The value of 0.015 eV found for the donor level in sample 1 (wet atmosphere) is lower than the corresponding value of sample 2 and other values reported in the literature for samples pyrolyzed in dry air at atmospheric pressure [10, 13].

The thermal treatment of the MnO_2 samples to temperatures above that of the pyrolytic decomposition results in an increase of the activation energy and the resistivity (see the corresponding $\log \rho$ versus $1/T$ curve for sample 3 in Fig. 3). This seems to indicate that the MnO_2 is a compensated semiconductor with electrons and holes as carriers, the hole concentration increasing with the thermal treatment. This hypothesis is supported by the fact that the α-Mn_2O_3 shows p-type semiconducting properties [13]. The proportion of both types of carriers in MnO_2 is probably related to the ratio of the concentrations of Mn(III) and Mn(IV), which cause the donor and acceptor levels respectively. It can also be observed that the samples pyrolyzed in a dry atmosphere have a resistivity about one order of magnitude higher than those pyrolyzed in wet air. This difference cannot be explained solely by the higher degree of compaction of the MnO_2 deposited in wet air and might be attributed to the higher reduction of the samples obtained in the dry atmosphere [10].

Samples 2 and 3 show an increasing activation energy from about 0.04 to 0.1 eV as the temperature is raised. This situation is typical of a temperature range in which there is an extrinsic–intrinsic transition in the electrical conduction (the transition is not shown by sample 1 in the temperature range investigated, due to the much larger number of carriers). These two samples, especially sample number 3, also show an inflexion

Table 1. Proportions of β- and γ-MnO_2 formed in various pyrolyses

Sample	*Treatment*	*β-MnO_2 (%)*	*γ-MnO_2 (%)*
1	Wet pyrolysis	53	47
2	Dry pyrolysis	48	52
3	Sample 1 heated to 350° C for 30 min in air	65	35
4	Sample 1 heated to 450° C for 30 min in air	74	26

Table 2. Values of room temperature resistivity and the slopes of the curves in Fig. 3.

Sample	*Resistivity at 20° C (Ω cm)*	*Slope (eV)*	*Temperature range (° C)*
1	0.4	0.015	−170–30
2	7.5	0.043–0.10	−122–250
3	21	0.040–0.10	−22–250
4	99×10^3	0.48	25–400

in the resistivity curve around 30° C. In this connection, it might be interesting to point out that MnO_2 shows a ferro- to paraelectric transition [14] at around this temperature (in the ferroelectric state the dielectric constant is above 10^5) which influences the electrical conductivity, as in the case of barium titanate.

Finally, sample 4, which consists of Mn_2O_3, has a variation of resisitivity with temperature that can be explained by assuming an intrinsic conduction in the high-temperature range. From the curve in Fig. 3, a value for the gap of 0.94 eV is obtained, which is in good agreement with that reported by Klose [13].

2.4. *Application to capacitor structures*

Planar capacitors of the TMM ($Ta-Ta_2O_5-MnO_2$-metal) type were prepared on a tantalum foil previously subjected to standard cleaning and chemical polishing procedures [15]. The tantalum was anodized in a 0.01% H_3PO_4 aqueous solution at a constant current density of 1 mA cm^{-2} until a formation voltage of 100 V was reached. For comparison purposes, the MnO_2 layer was deposited by pyrolysis in both moist and dry air atmospheres as has been described before. The manganese nitrate was previously heated to 100° C so that a certain amount of water would evaporate. In this way the solution acquires a high viscosity and easily adheres to the smooth Ta_2O_5 film. After the pyrolytic deposition of the MnO_2 layer, the structure was re-anodized at 55 V in an HNO_3 electrolyte ($\rho = 800\,\Omega$ cm) following the procedures for the fabrication of tantalum capacitors. Finally, electrical contacts were attached using a silver paste.

The low-frequency capacitance of both types of capacitors was about 0.13 μF cm^{-2}. Fig. 4 shows the frequency variation of the capacitance, referred to its value at 100 Hz, and the dissipation factor tan δ, which were measured with a General Radio 1620 capacitance bridge. The strong dispersion in capacitance and losses shown by the capacitors with the MnO_2 layer deposited in dry air can be attributed to their higher contact resistance R_c. In effect, the values obtained for R_c, following the series analysis of McLean [16], were 0.50 Ω and 17.8 Ω for the capacitors in which the MnO_2 was obtained in moist and dry atmospheres

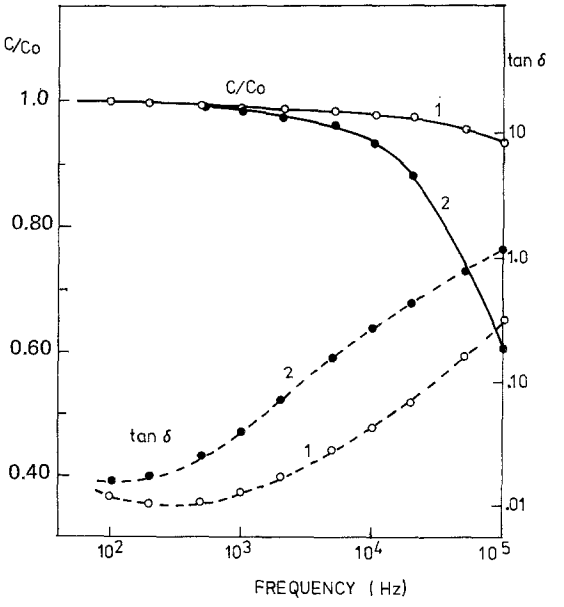

Fig. 4. Variation of relative capacitance (full line) and tan δ (broken line) with frequency for tantalum capacitors with MnO_2 deposited in humid (curve 1) and dry (curve 2) atmospheres.

respectively. This fact can be explained if we take into account the higher porosity of the surface and the larger resistivity of the MnO_2 layers deposited in dry air.

The leakage current was measured in a 10% H_3PO_4 aqueous electrolyte after polarizing the capacitors for 5 minutes at one-quarter the formation voltage ($V_f = 100$ V). A value of about 10^{-7} A cm^{-2} was obtained for the samples with the MnO_2 deposited in moist air, and a value one order of magnitude larger for the corresponding ones prepared in a dry atmosphere. In both cases, the variation of the leakage current across the TMM structure, besides being nonlinear, presented a strong rectifying character. Under cathodic polarization, the current increased very abruptly for voltages higher than 12 V, which can be considered as the maximum-rated positive voltage to be applied to the cathode in these capacitors. For positive voltages applied to the anode, the leakage current increased as the square root of the applied voltage. From the slope of this curve a conduction mechanism of the Poole–Frankel type is obtained, which agrees with that reported by Klein [17] in similar structures.

The measurement of the scintillation voltage V_s of the capacitors during the re-anodization process

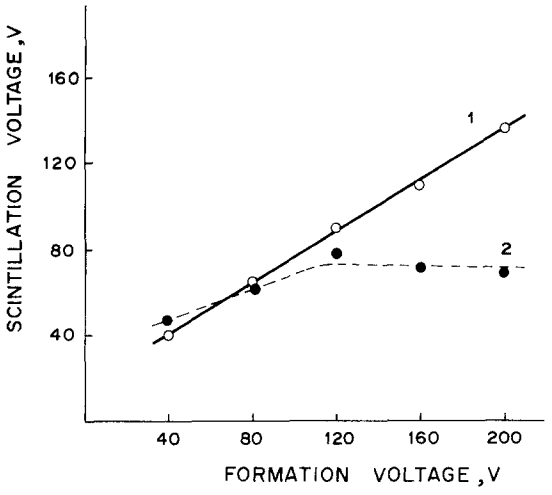

Fig. 5. Scintillation voltages during the re-anodization process in tantalum capacitors with MnO_2 deposited in humid (curve 1) and dry (curve 2) atmospheres.

is meaningful, not only because this puts a limit on the maximum voltage to be applied in the re-oxidation, but also because it is related to the nominal working voltage of the capacitor. In order to measure V_s several capacitors with formation voltages between 40 and 200 V were prepared with MnO_2 deposited in both wet and dry atmospheres. These capacitors were then re-oxidized at a constant current density of 1 mA cm^{-2} and the voltage was left to increase until the scintillation or breakdown phenomenon first appeared. Fig. 5 shows the scintillation voltage of the capacitors as a function of the initial anodization voltage, each point representing the average for three similar capacitors. For low formation voltages, V_f below 120 V, the scintillation voltage shows a linear variation for both kinds of capacitors (Fig. 5, curves 1 and 2 for the capacitors with the MnO_2 layer deposited in wet and dry atmospheres respectively). For higher values of V_f, the capacitors obtained in moist air still show a scintillation voltage linearly increasing with the formation voltage, whereas the capacitors obtained in a dry atmosphere present a maximum scintillation voltage between 70 and 80 V. This fact coincides with the usual industrial practice of setting a limit of 65 V on the reoxidation voltage, even for the capacitors with the highest formation voltages. The lower value found for V_s with respect to V_f in curve 1 might be explained in terms of the damage produced in the Ta_2O_5 during the pyrolysis and the difficulty which the electrolyte finds, throughout the reoxidation process [18], in supplying oxygen atoms to the Ta_2O_5 across the MnO_2 layer. The results of curve 2 are more difficult to explain, although the larger leakage current obtained for these capacitors shows that, according to the theory proposed by Klein and Jaeger [17], there is a correlation between the ionic and electronic currents, the latter being higher as the oxidation degree of the semiconductor layer decreases. The resisitivity measurements of the MnO_2 samples and the I–V characteristics of the TMM structures reported in this work further support this view. The lack of experimental results in this field, as well as the absence of an appropriate theory of the scintillation phenomenon [19, 20], greatly hampers the finding of a definite explanation.

3. Summary and conclusions

Although the deposition of the MnO_2 by pyrolysis in moist and dry atmospheres follows very similar kinetics, the properties of the resulting products are substantially different. In particular, the grain size at the surface and the electrical resistivity are profoundly affected. The larger resistivity of the MnO_2 layers obtained in a dry atmosphere has been explained in terms of the lower oxygen content of the MnO_2 grains. As a result, the tantalum capacitors employing this kind of electrolyte show a considerable contact resistance which strongly affects their high-frequency performance. At the same time, these capacitors show a larger leakage current and a lower scintillation voltage in the re-oxidation process than those with the MnO_2 layer obtained by pyrolysis in an atmosphere saturated with water vapour.

Acknowledgements

We would like to acknowledge the Spanish Comisión Asesora de Investigación Científica y Técnica and Piher S. A. (Barcelona, Spain) for partial support of this work.

References

[1] D. M. Smyth, G. A. Shirn and T. B. Tripp, *J. Electrochem. Soc.* **110** (1963) 1264.
[2] T. Takagi, F. Eguchi, H. Kihara-Morishita and T. Takamura, *Denki Kagaku* **44** (1976) 713.

[3] See, for example, references cited in the paper of W. J. Bernard, *J. Electrochem. Soc.* **124** (1977) 403C.
[4] F. F. Zind, US Patent 3337 429 (1967).
[5] H. Bub, K. Gottschämmer and H. Spiess, German Patent 1935 002 (1971).
[6] J. M. Albella, L. Fernández-Navarete, J. M. Martínez-Duart, *J. Electrochem. Soc.* **127** (1980) 2180.
[7] P. K. Gallagher, F. Scherey and B. Prescott, *Thermochim. Acta* **2** (1971) 405.
[8] P. K. Gallagher and D. W. Johnson, *ibid* **2** (1971) 413.
[9] *Idem, J. Electrochem. Soc.* **118** (1971) 1530.
[10] S. S. Wiley and H. T. Knight, *ibid* **111** (1964) 656.
[11] E. Preisler, *J. Appl. Electrochem.* **6** (1976) 311.
[12] M. G. Bodas, H. V. Keer and A. B. Biswas, *J. Ind. Chem. Soc.* **52** (1975) 221.
[13] P. H. Klose, *J. Electrochem. Soc.* **117** (1970) 854.
[14] V. G. Bhide and R. V. Damle, *Physica* **26** (1960) 33.
[15] J. M. Albella, I. Montero and J. M. Martínez-Duart, *Thin Solid Films* **58** (1979) 307.
[16] D. A. McLean, *J. Electrochem. Soc.* **108** (1961) 48.
[17] G. P. Klein and N. I. Jaeger, *Thin Solid Films* **46** (1977) 103.
[18] D. M. Smyth, *J. Electrochem Soc.* **113** (1966) 19.
[19] V. Kadary and N. Klein, *ibid* **127** (1980) 139.
[20] J. M. Martínez-Duart, J. M. Albella and J. Baonza, *Thin Solid Films* **36** (1976) 371.